IJE TRANSACTIONS B: Applications Vol. 27, No. 2, (February 2014) 215-226

International Journal of Engineering

Journal Homepage: www.ije.ir

Entropy Generation of Double Diffusive Natural Convection in a Three Dimensional Differentially Heated Enclosure

CH. Maatki*, K. Ghachem, L. Kolsi, M. N. Borjini, H. Ben Aissia

Department of Energetic, University of Monastir, Monastir, Tunisie

PAPER INFO

Paper history:
Received 10 April 2013
Accepted in revised form 20 June 2013

Keywords:
Entropy Generation
Double Diffusion
Natural Convection
Energy
Three Dimensional

ABSTRACT

Entropy generation of double diffusive natural convection in a three dimensional differentially heated enclosure has been performed numerically. Vertical walls of enclosure are heated differentially and remaining walls are adiabatic. The obtained results were presented via iso-concentration, iso-temperatures, velocity vector projection, particle trajectories, velocity profiles, iso-entropy, local Nusselt and Sherwood numbers, average Nusselt and Sherwood numbers and Bejan numbers at different value of buoyancy ratio ($-2 \le N \le 2$) and Rayleigh numbers ($10^3 \le Ra \le 10^5$). The Lewis number is fixed at Le = 2. It is found that both Rayleigh number and buoyancy ratio play dominant role on entropy generation and heat and mass transfer as well as fluid flow. A special case occurred between $-1.5 \le N \le -1$ and complex structure is observed.

doi: *10.5829/idosi.ije.2014.27.02b.06*

NOMENCLATURE

Be	Bejan number
C	Dimensionless concentration
D	Mass diffusivity
Gr	Grashof number
K	Thermal conductivity
Le	Lewis Number
N	Buoyancy ratio
N_s	Local generated entropy
Pr	Prandtl number
Ra	Rayleigh number
Sc	Schmidt number
Sh	Sherwood number
S'_{gen}	Generated entropy
t	Dimensionless time
T	Dimensionless temperature
T'_c	Cold temperature
T'_h	Hot temperature
$\vec{V}$	Dimensionless velocity vector
W	Enclosure width

Greek Symbols

α	Thermal diffusivity
β	Expansion coefficient
μ	Dynamic viscosity
ν	Kinematic viscosity
υ_0	Characteristic speed of fluid ($=\alpha / W$)
$\varphi_1, \varphi_2, \varphi_3$	Irreversibilities coefficients
ϕ'	Dissipation function
$\vec{\psi}$	Dimensionless vector potential
$\vec{\omega}$	Dimensionless vorticity

Superscripts

x,y,z	Cartesian coordinates
dif	Diffusive
fr	Friction
th	Thermal
tot	Total

Subscripts

'	Dimensional variable

*Corresponding Author Email: maatkichems@yahoo.fr (CH. Maatki)

1. INTRODUCTION

The effect of buoyancy ratio on the flow structure is investigated numerically for a binary mixture gas in a rectangular enclosure by Nishimura et al. [1]. They indicated that the key mechanism for oscillatory flow is that the unstably stratified region of species shifts from the central part of the enclosure to the upper and lower parts, and vice versa in a time-periodic sense, due to the interaction of heat and mass transfer with different diffusivities near the vertical walls.

The simultaneous heat and mass transfer by natural convection in an air-filled cavity of aspect ratio 7.0 is investigated numerically and experimentally for both a horizontal and vertical cavity by Wee et al. [2]. The finite-difference equations are solved by the dynamic alternating direction implicit (DADI) method. Transient, double diffusive natural convection in a horizontal enclosure is investigated in an enclosure numerically and analytically by Bennacer et al. [3]. Bennacer and Gobin [4, 5] made a study on double diffusive natural convection in a binary fluid contained in a two-dimensional enclosure where horizontal temperature and concentration differences are specified. They proposed a general mass transfer correlation which is valid over a wide range of parameters. A three-dimensional numerical study had been performed using vorticity-vector potential formulations based on the finite-volume method to investigate the double-diffusive convection in a stack of cubic enclosures. Their result showed that the effect of heat and mass diffusive walls differs between the case of thermally dominated flow and the compositionally dominated one. Papanicolaou and Belessiotis [6] worked on natural convective heat and mass transfer in an asymmetric, trapezoidal enclosure. Steady-state thermosolutal convection in a square cavity filled with air, submitted to horizontal temperature and concentration gradients, is studied numerically by Béchein et al. [7]. They obtained correlations between heat and mass transfer rates and the non-dimensional numbers characterizing the flow phenomena. Sezai and Mohamad [8] made a numerical study on double diffusive convection in a cubic enclosure with opposing temperature and concentration gradients. The flow is driven by buoyancy forced due to temperature and solutal gradients. They stated that the double diffusive flow in enclosures with opposing buoyancy forces is strictly three dimensional for a certain range of parameters. Hyun and Lee [9] studied the double-diffusive convection in a rectangular cavity, numerically. They presented the mean Sherwood and mean Nusselt number for different value of buoyancy ratio. Other studies on natural convection of double diffusive natural convection problem can be found in literature as Goyeau et al. [10]. Murty et al. [11] was used to finite element method to solve double diffusive convection problem. Other studies related with double diffusion problem can be found in literature as Chen and Du [12] and Han and Kuehn [13], Reena and Rana [14], Borjini et al. [15] and Jaimal et al. [16].

Calculation of entropy generation in an energetical system is important to find the energy losses and enhances the energy efficiency in the system. Bejan [17-20] proposed the entropy generation minimization technique and it may apply for many systems such as high velocity pipe flow [21], natural convection under magnetic field [22], binary gas mixture of mixed convection [23], natural convection in different shaped cavities [24-26], porous medium [27, 28]. Some review [29] and fundamental studies [30, 31] are performed on this subject. However, entropy generation on double diffusive natural convection heat transfer is very limited. In this context, Chen and Du [12] investigated the effects of thermal Rayleigh number, ratio of buoyancy forces and aspect ratio on entropy generation of turbulent double-diffusive natural convection in a rectangle cavity. They found that total entropy generation increases with Rayleigh number, aspect ratio and values of N>1.

The main objective of the present work is to examine the entropy generation in a three dimensional double diffusive natural convection. Based on literature survey, there is no study on entropy generation due to natural convection in three dimensional cavities.

2. PROBLEM FORMULATION

Studied model is presented in Figure 1. It is three dimensional models for an enclosure under different temperature of vertical walls and remaining walls are adiabatic. Gravity acts in vertical y direction. It is filled with binary fluid mixture and Prandtl number is chosen a 0.7 for whole work.

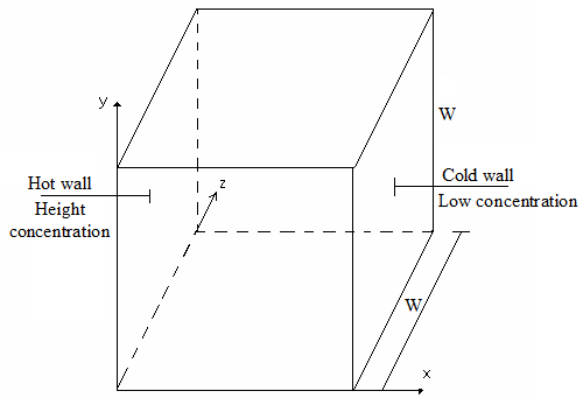

Figure 1. Schematic diagram of the physical system

The equations describing the double diffusive natural convection are the equations of continuity Equation (1), of momentum Equation (2), of energy Equation (3) and species diffusion Equation (4):

$$\nabla.\vec{V}'=0 \tag{1}$$

$$\frac{\partial \vec{V}'}{\partial t'}+(\vec{V}'.\vec{\nabla})\vec{V}'=-\frac{1}{\rho}\vec{\nabla}P'+\nu\Delta\vec{V}'+\beta_t(T'-T_0)\vec{g}+\beta_c(C'-C_0)\vec{g} \tag{2}$$

$$\frac{\partial T'}{\partial t'}+\vec{V}'.\nabla T'=\alpha\nabla^2 T' \tag{3}$$

$$\frac{\partial C'}{\partial t'}+\vec{V}'.\nabla C'=D\nabla^2 C' \tag{4}$$

As numerical method, we had recourse to the vorticity-vector potential formalism $(\vec{\psi}-\vec{\omega})$ which allows, in a three dimensional configuration, the elimination of the pressure, which is a delicate term to treat. To eliminate this term, one applies the rotational to the equation of momentum. The vector potential and the vorticity are defined by the two following relations:

$$\vec{\omega}'=\vec{\nabla}\times\vec{V}' \text{ and } \vec{V}'=\vec{\nabla}\times\vec{\psi}' \tag{5}$$

In the Equations (1) to (4), time t', velocity $\vec{V}'$, the vector potential $\vec{\psi}'$, the vorticity $\vec{\omega}'$ are put in their adimensional forms by W^2/α, α/W, α and W^2/α, respectively. The dimensional temperature and concentration are defined by:

$$T=\frac{(T'-T'_c)}{(T'_h-T'_c)} \text{ and } C=\frac{(C'-C'_l)}{(C'_h-C'_l)}.$$

After application of the $(\vec{\psi}-\vec{\omega})$ formalism and adimensionalisation, the system of equations controlling the phenomenon becomes:

$$-\vec{\omega}=\nabla^2\vec{\psi} \tag{6}$$

$$\frac{\partial\vec{\omega}}{\partial t}+(\vec{V}.\nabla)\vec{\omega}-(\vec{\omega}.\nabla)\vec{V}=\Delta\vec{\omega}+Ra.\Pr.\left[\frac{\partial T}{\partial z}-N\frac{\partial C}{\partial z};0;-\frac{\partial T}{\partial x}+N\frac{\partial C}{\partial x}\right] \tag{7}$$

$$\frac{\partial T}{\partial t}+\vec{V}.\nabla T=\nabla^2 T \tag{8}$$

$$\frac{\partial C}{\partial t}+\vec{V}.\nabla C=\frac{1}{Le}\nabla^2 C \tag{9}$$

Dimensionless variables are :

$$\Pr=\frac{\nu}{\alpha},\quad Ra=\frac{g.\beta_t.W^3.(T'_h-T'_c)}{\alpha.\nu},\quad N=\frac{\beta_c.(C'_h-C'_l)}{\beta_t.(T'_h-T'_c)},\quad Le=\frac{\alpha}{D}=\frac{Sc}{\Pr} \tag{10}$$

The control volume finite difference method [32] is used to discretize Equations (6) to (9). The central-difference scheme for treating convective terms and the fully implicit procedure to discretize the temporal derivatives are retained. The grid is uniform in all directions with additional nodes on boundaries. The successive relaxation iterating scheme [32] is used to solve the resulting non-linear algebraic equations.
The boundary conditions are given as:

- Temperature

$$T=1 \text{ at } x=1,\ T=0 \text{ at } x=0;\quad \frac{\partial T}{\partial n}=0 \text{ on other walls (adiabatic).} \tag{11}$$

- Concentration

$$C=1 \text{ at } x=1,\ C=0 \text{ at } x=0;\quad \frac{\partial C}{\partial n}=0 \text{ on other walls (impermeable).} \tag{12}$$

- Vorticity

$$\omega_x=0,\ \omega_y=-\frac{\partial V_z}{\partial x},\ \omega_z=\frac{\partial V_y}{\partial x} \text{ at } x=0 \text{ and } 1$$

$$\omega_x=\frac{\partial V_z}{\partial y},\ \omega_y=0,\ \omega_z=-\frac{\partial V_x}{\partial y} \text{ at } y=0 \text{ and } 1 \tag{13}$$

$$\omega_x=-\frac{\partial V_y}{\partial z},\ \omega_y=\frac{\partial V_x}{\partial z},\ \omega_z=0 \text{ at } z=0 \text{ and } 1$$

- Vector potential

$$\frac{\partial\psi_x}{\partial x}=\psi_y=\psi_z=0 \text{ at } x=0 \text{ and } 1$$

$$\psi_x=\frac{\partial\psi_y}{\partial y}=\psi_z=0 \text{ at } y=0 \text{ and } 1 \tag{14}$$

$$\psi_x=\psi_y=\frac{\partial\psi_z}{\partial z}=0 \text{ at } z=0 \text{ and } 1$$

- Velocity

$$V_x=V_y=V_z=0 \text{ on all walls} \tag{15}$$

Local Nusselt and Sherwood numbers are given as follows :

$$Nu=\left.\frac{\partial T}{\partial x}\right|_{x=0,1};\quad Sh=\left.\frac{\partial C}{\partial x}\right|_{x=0,1} \tag{16}$$

$$S'_{gen}=\left\{\frac{k}{T_0^2}\left[\left(\frac{\partial T'}{\partial x'}\right)^2+\left(\frac{\partial T'}{\partial y'}\right)^2+\left(\frac{\partial T'}{\partial z'}\right)^2\right]\right\}+\frac{\mu}{T_0}\left\{2\left[\left(\frac{\partial V'_x}{\partial x'}\right)^2+\left(\frac{\partial V'_y}{\partial y'}\right)^2+\left(\frac{\partial V'_z}{\partial z'}\right)^2\right]+\left(\frac{\partial V'_y}{\partial x'}+\frac{\partial V'_x}{\partial y'}\right)^2+\left(\frac{\partial V'_z}{\partial y'}+\frac{\partial V'_y}{\partial z'}\right)^2+\left(\frac{\partial V'_x}{\partial z'}+\frac{\partial V'_z}{\partial x'}\right)^2\right\}$$
$$+\left\{\frac{RD}{C_0}\left[\left(\frac{\partial C'}{\partial x'}\right)^2+\left(\frac{\partial C'}{\partial y'}\right)^2+\left(\frac{\partial C'}{\partial z'}\right)^2\right]+\frac{RD}{T_0}\left[\left(\frac{\partial T'}{\partial x'}\right)\left(\frac{\partial C'}{\partial x'}\right)+\left(\frac{\partial T'}{\partial y'}\right)\left(\frac{\partial C'}{\partial y'}\right)+\left(\frac{\partial T'}{\partial z'}\right)\left(\frac{\partial C'}{\partial z'}\right)\right]\right\} \quad (18)$$

$$N_S=\left[\left(\frac{\partial T}{\partial x}\right)^2+\left(\frac{\partial T}{\partial y}\right)^2+\left(\frac{\partial T}{\partial z}\right)^2\right]+\varphi_1\left\{2\left[\left(\frac{\partial V_x}{\partial x}\right)^2+\left(\frac{\partial V_y}{\partial y}\right)^2+\left(\frac{\partial V_z}{\partial z}\right)^2\right]+\left[\left(\frac{\partial V_y}{\partial x}+\frac{\partial V_x}{\partial y}\right)^2+\left(\frac{\partial V_z}{\partial y}+\frac{\partial V_y}{\partial z}\right)^2+\left(\frac{\partial V_x}{\partial z}+\frac{\partial V_z}{\partial x}\right)^2\right]\right\}$$
$$+\left\{\varphi_2\left[\left(\frac{\partial C}{\partial x}\right)^2+\left(\frac{\partial C}{\partial y}\right)^2+\left(\frac{\partial C}{\partial z}\right)^2\right]+\varphi_3\left[\left(\frac{\partial T}{\partial x}\right)\left(\frac{\partial C}{\partial x}\right)+\left(\frac{\partial T}{\partial y}\right)\left(\frac{\partial C}{\partial y}\right)+\left(\frac{\partial T}{\partial z}\right)\left(\frac{\partial C}{\partial z}\right)\right]\right\} \quad (19)$$

The average values of Nusselt and Sherwood numbers, on the isothermal walls are expressed by:

$$\overline{Nu}=\int_0^1\int_0^1 Nu.\partial y.\partial z \quad \overline{Sh}=\int_0^1\int_0^1 Sh.\partial y.\partial z \quad (17)$$

The local entropy generation rate in a three-dimensional flow with single diffusing specie of concentration (C) can be written [30] as Equation (18); where, C_0 and T_0 are the reference concentration and temperature, respectively. After adimensionalisation, we obtain the dimensionless local generated entropy as [30] Equation (19). The first term of N_s represents the thermal irreversibility which is noted $N_{S\text{-}th}$. The second term represents the viscous irreversibility which is noted $N_{S\text{-}fr}$ and the third term represents the diffusive irreversibility which is noted $N_{S\text{-}dif}$. N_S give a good idea on the profile and the distribution of the generated local dimensionless entropy. The average dimensionless generated entropy is written:

$$S_{tot}=\frac{1}{V}\int_v N_s dv=\frac{1}{V}\int_v\left(N_{s-th}+N_{s-fr}+N_{s-dif}\right)dv$$
$$S_{tot}=S_{th}+S_{fr}+S_{dif} \quad (20)$$

Dimensionless irreversibilities distribution ratios (φ_1, φ_2 and φ_3), are given by:

$$\varphi_1=\frac{\mu\alpha^2 T_0}{L^2 k\Delta T^2};\quad \varphi_2=\frac{RDT_0}{kC_0}\left[\frac{\Delta C'}{\Delta T'}\right]_{\text{and}}\quad \varphi_3=\frac{RD}{k}\left[\frac{\Delta C'}{\Delta T}\right] \quad (21)$$

Mean Bejan number is defined as :

$$Be=\frac{S_{th}+S_{dif}}{S_{th}+S_{dif}+S_{fr}} \quad (22)$$

3. RESULTS AND DISCUSSIONS

Heat and fluid flow and entropy generation of double diffusive natural convection in a three dimensional differentially heated enclosures were investigated numerically for different parameters. Results will be presented in this part of the study via isocontcentration, iso-temperatures, velocity vector projection, particle trajectories, velocity profiles, iso-entropy, local Nusselt and Sherwood numbers, average Nusselt and Sherwood numbers and Bejan numbers. Results are presented in two different subtitles as thermal and flow field and also entropy generation.

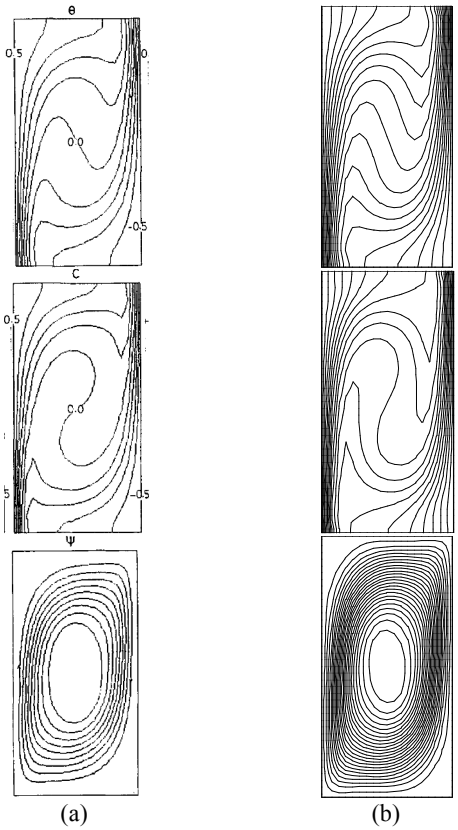

(a) (b)

Figure 2. Comparison of the isotherm, isoconcentration and z-vector potential plots in the X-Y plan by Nishimura et al. [1] at Ra = 10^5, N=0.8 and AR = 2.0, (a) Nishimura, et al. [1] and (b) Present Code

3. 1. Grid Sensitivity Check and Code Validation

The first simulations are carried for N= -0.5, Le=2, Pr = 0.7, and Ra = 10^5 in order to choose adequate spatial meshes. A dimensionless time step equal to 10^{-4} is retained. Results justifies quantitatively the use of 51x51x51 spatial meshes, at least for Ra=10^5. A validation has been performed between present study and studies of Nishimura et al. [1]. In this context, Figure 2 illustrates the isotherm, iso-concentration and z-vector potential by comparing present results (on the right column) and Nishimura's results (on the left). As seen from the figure, obtained results show good agreement with literature.

3. 2. Flow and Thermal Fields

As indicated in the literature, when buoyancy ratio less than unity, the flow is primarily dominated by the thermal buoyancy force and for buoyancy ratio greater than 1, the compositional buoyancy force rather than the thermal buoyancy force dominates the flow. Figure 3 shows isotherms for six different values of buoyancy ratio at different Rayleigh numbers. On the left side, values are given for positive and right column negative. As seen from the figure, variation of buoyancy values is not effective near vertical walls for all values of Rayleigh numbers. For Ra = 10^3, conductive mode of heat transfer becomes dominant. Intersection point among buoyancy ratio goes down and show diagonal variation for positive values. However, intersection points become almost same along a line. When N = -1, isotherms are almost constant. In other words, they exhibit a parallel distribution to the vertical walls. As an interesting result, there are no huge differences on isotherms for positive values of buoyancy ratios. On the other hand, negative values of buoyancy ratio are more effective on isotherms.

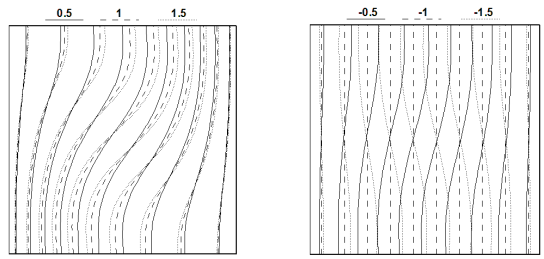

(a)

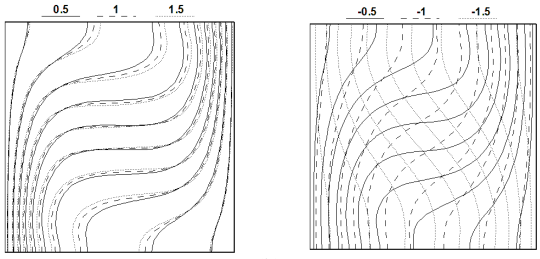

(b)

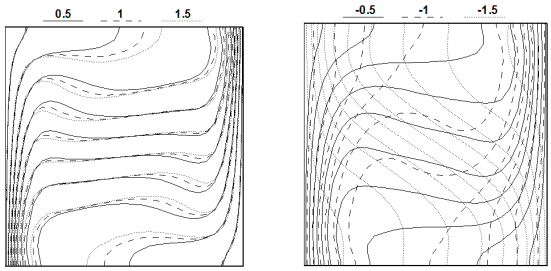

(c)

Figure 3. Iso-temperature for different Rayleigh number in (x-y) planes a) Ra = 10^3, b) Ra = 10^4, c) Ra = 10^5

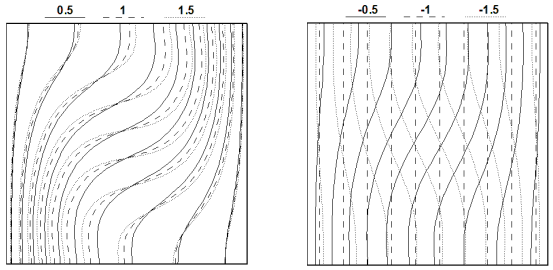

(a)

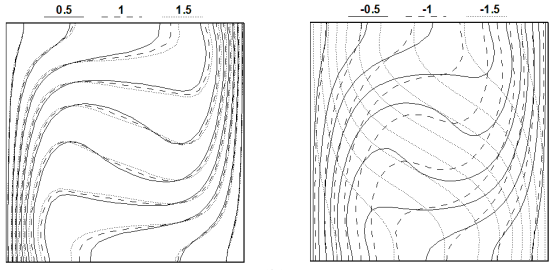

(b)

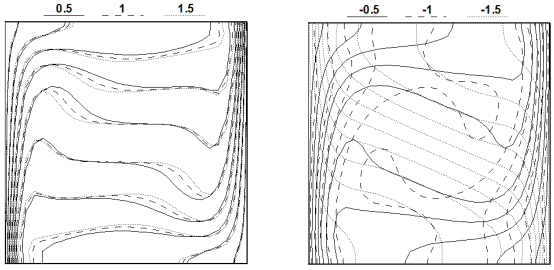

(c)

Figure 4. Iso-concentration for different Rayleigh number for in (x-y) planes, a) Ra = 10^3, b) Ra = 10^4, c) Ra = 10^5

For N = -1.5, isotherms present a completely different distributions than others. For the same studied parameters, iso-concentration plots are given in Figure 4. Iso-concentration contours show regular distribution for low Rayleigh number even at core region. However, the concentration contours are furthermore distorted in the core especially at higher value of Rayleigh number. This result is supported by

Nishimura et al. [1]. This is clearly seen from three-dimensional visualizations as given in Figure 5 at N = -1. In this case, species diffusivity is being half the thermal diffusivity. Again, as seen from Figure 5, regular distribution on iso-concentration occurs for N = 1 and N = -1.5.

In addition, variation of buoyancy ratio is effective on velocities as seen from Figure 6. The figure also shows the vector velocity projection in the central plan (z = 0.5) at Ra = 10^5. For most cases (N = 0.5, 1, 1.5, -0.5 and -1.5), two cells were formed near right top and left bottom sides. Furthermore, another cell appears at the middle for N = -2 and 2. It is an interesting result that N = 1 shows different distribution on flow. Number of cell decreases with decreasing of Rayleigh number for each values of buoyancy ratio as seen from Figures 7 and 8. Velocity shows special variations at N = -1 for each values. Locations of corner cells change with Ra = 10^4 and four different cells were observed at Ra = 10^3.

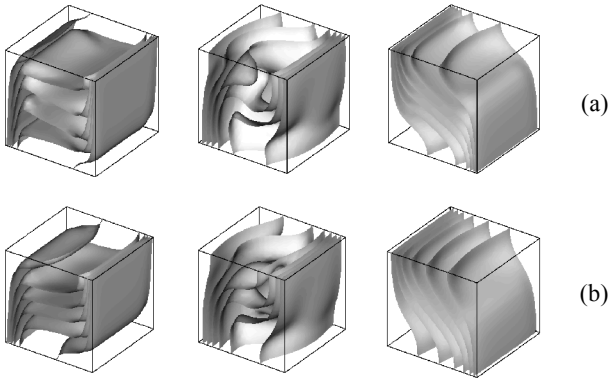

Figure 5. (a) Iso-surfaces of concentration (on the top row), (b) Iso-surfaces of temperature (on the bottom wall) for Ra=10^5 and buoyancy ratio

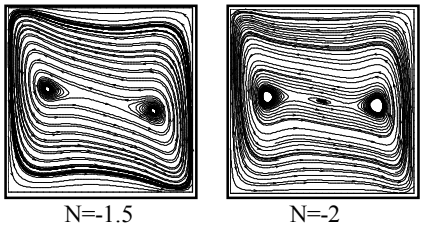

Figure 6. Vector velocity projection in the central plan (z=0.5) for Ra=10^5 and different buoyancy ratio

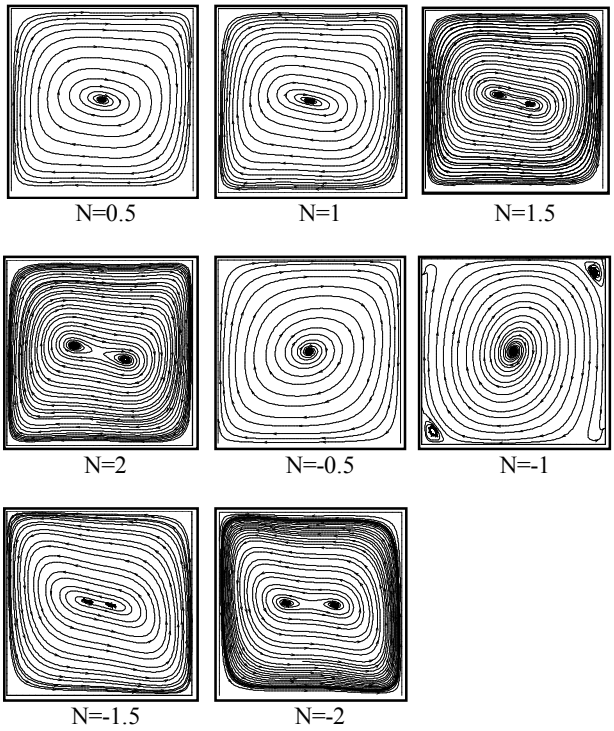

Figure 7. Vector velocity projection in the central plan (z=0.5) for Ra=10^4 and different buoyancy ratio

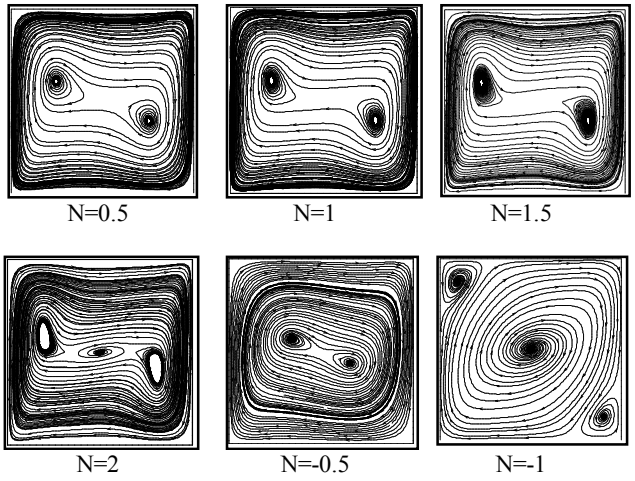

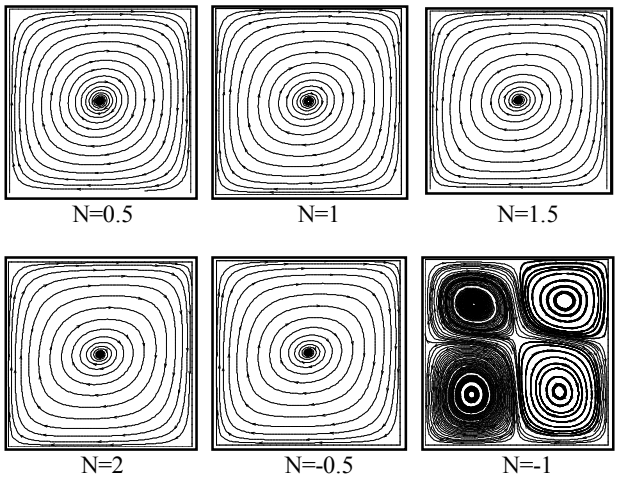

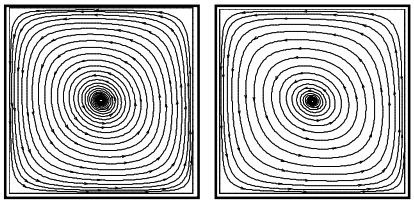

Figure 8. Vector velocity projection in the central plan (z=0.5) for Ra=10^3 and different buoyancy parameter

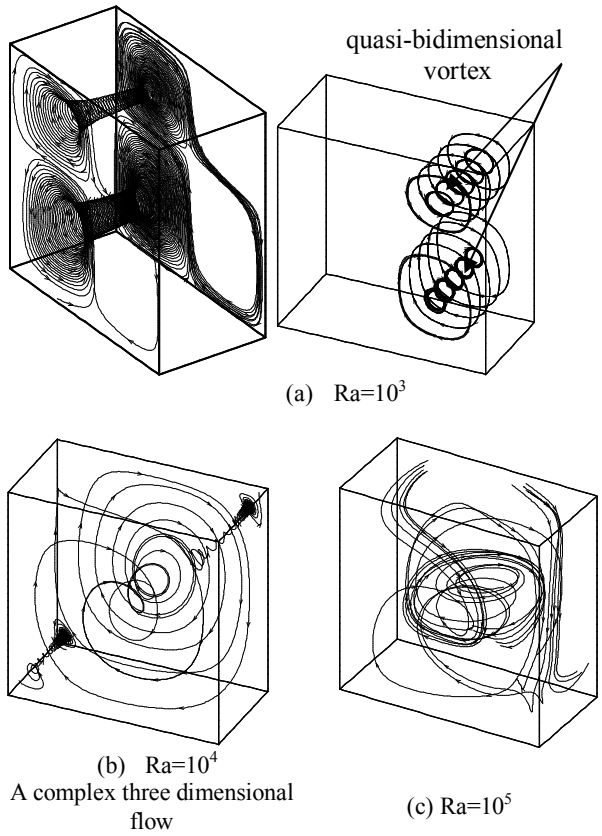

Figure 9. Some Particles trajectories for N=-1, a) Ra = 10^3, b) Ra = 10^4, c) Ra = 10^5

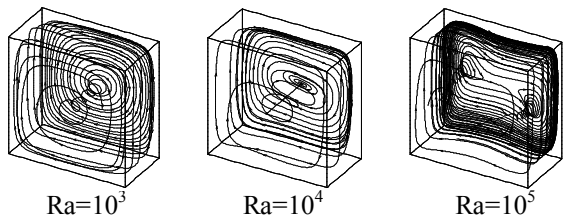

Figure 10. Some Particles trajectories for N = 1, a) Ra = 10^3, b) Ra = 10^4, c) Ra = 10^5

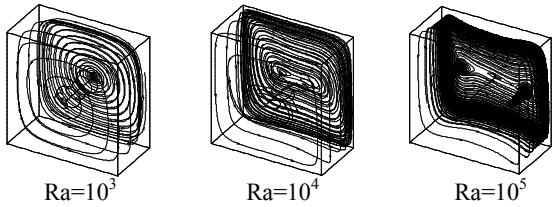

Figure 11. Some Particles trajectories for N = 2, a) Ra = 10^3, b) Ra = 10^4, c) Ra = 10^5

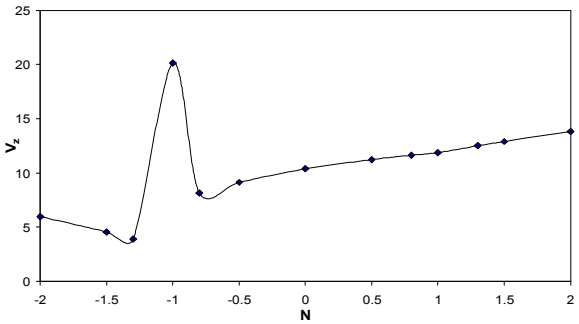

Figure 12. Velocity component V_z as function of N at Ra=10^5

The complexity for N = -1 can be explained via three dimensional visualization of some particle trajectories as shown in Figure 9 for different Rayleigh numbers. To compare and see the effects of buoyancy ratio on particle trajectories, two different cases are plotted for N = 1 (Figure 10) and N = 2 (Figure 11). For Ra = 10^5, velocity profiles are plotted versus buoyancy ratio in Figure 12. As seen from the figure, velocity value becomes maximum for N = -1 and it increases linearly with increasing of N values.

3. 3. Heat and Mass Transfer Characteristics

Heat transfer results are presented via local and average Nusselt numbers and mass transfer is given by Sherwood numbers. Variation of local Nusselt numbers are given by contours in Figure 13 for Ra = 10^5 and N=1, -0.5, -1 and -2. Nusselt number values are decreased with decreasing of buoyancy ratio. For N = 1 and -0.5, local Nusselt number decreases from bottom to top and a complex distribution is formed. Distribution of Sherwood numbers exhibit opposite variation as seen in Figure 14 for Ra = 10^5. Sherwood numbers are decreased from top to bottom for N = 1 and N = -0.5. An opposite distribution is occurred for the case of N = -2. A closed chamber is located near the top wall. Figure 15 (a) and (b) illustrate the mean Nusselt and mean Sherwood numbers, respectively. For Ra = 10^3, both mean *Nu* and mean *Sh* are almost unity for all values of N due to domination of conduction mode of heat transfer. A minimum values

are formed around N = -1 for both calculations and it increases with increasing of N values. Both figures show that heat and mass transfer increase with N values.

3. 4. Entropy Generation Entropy generation is calculated from its definition after calculations of velocities, concentrations and temperatures. The irreversibilities coefficients are fixed at $\varphi_1 = 10^{-4}$, $\varphi_2 = 0.5$ and $\varphi_3 = 10^{-2}$ respectively for all studied cases. In convective heat and mass transfer and for a non reactive mixture, irreversibility arises due to the heat transfer, the viscous effects and the mass transfer. The entropy generation rate is expressed as the sum of contributions due to thermal, viscous and diffusive effects. Thus, it depends functionally on the local values of temperature, velocity and concentration in the domain of interest [17]. In other words, the local entropy generation rate is a function of temperature and velocity gradients in the x and y directions in the entire calculation. Hence, it is a good indicator of grid dependence.

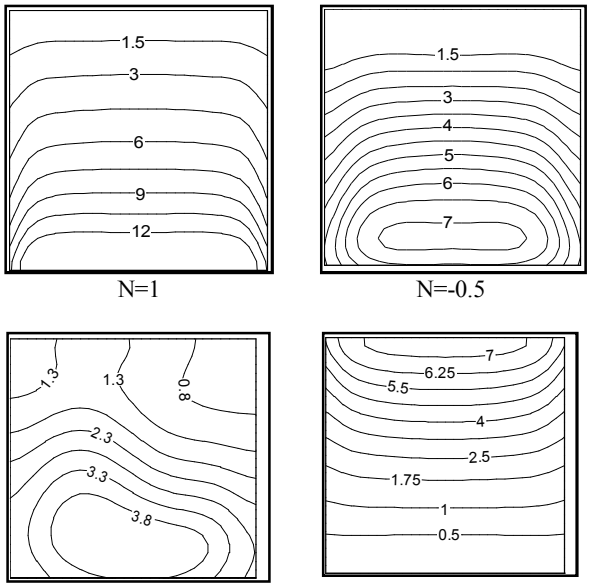

N=1 N=-0.5

N=-1 N=-2

Figure13. Local Nusselt number for $Ra=10^5$

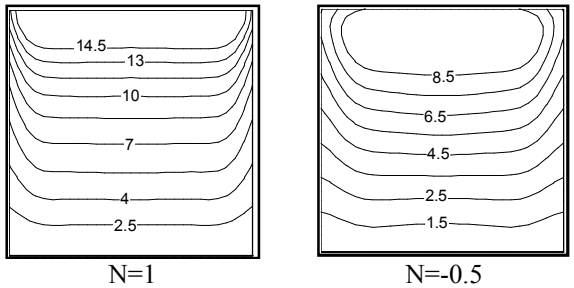

N=1 N=-0.5

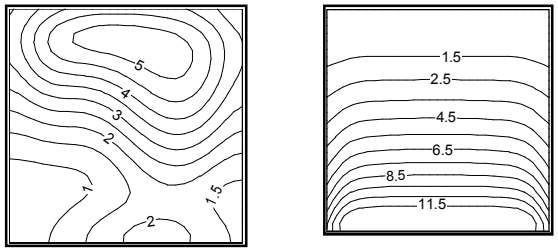

N=-1 N=-2

Figure 14. Local Sherwood number for $Ra=10^5$

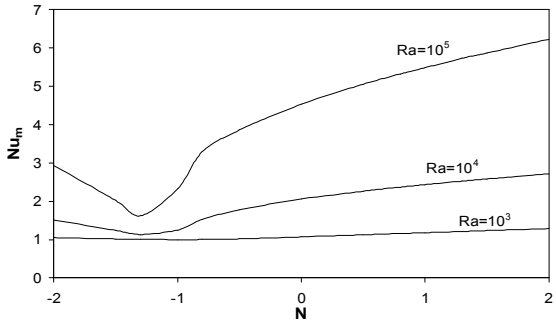

(a)

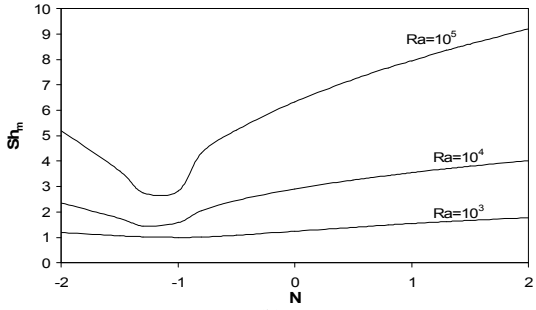

(b)

Figure 15. a) Average Nusselt number as function of N, b) Average Sherwood number as function of N

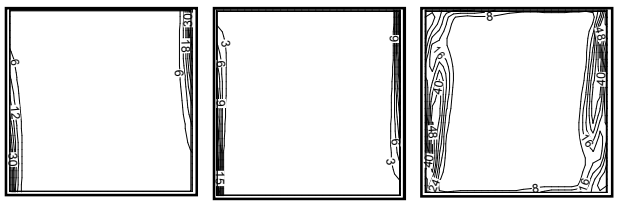

Thermal Diffusive Friction

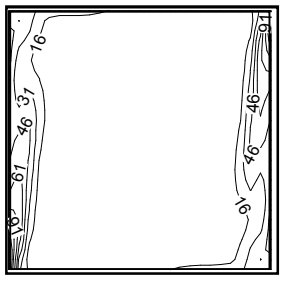

Total

Figure 16. Iso-Entropy for N=1, $Ra=10^5$, $\varphi_1=10^{-4}$, $\varphi_2=0.5$ and $\varphi_3=0.01$

In this part of the study, entropy results are presented via entropy generation due to temperature, entropy generation due to diffusion, entropy generation due to friction and total entropy generation. For N = 1 and Ra = 10^5, entropy contours are plotted in Figure 16. The heat transfer irreversibilities and the diffusive irreversibilities are found similar and mainly confined to the lower and the upper corners of the heated and the cooled walls. This result is supported by Maghrebi et al. [30]. Entropy generation due to fluid friction is effective on vertical walls and half of horizontal walls.

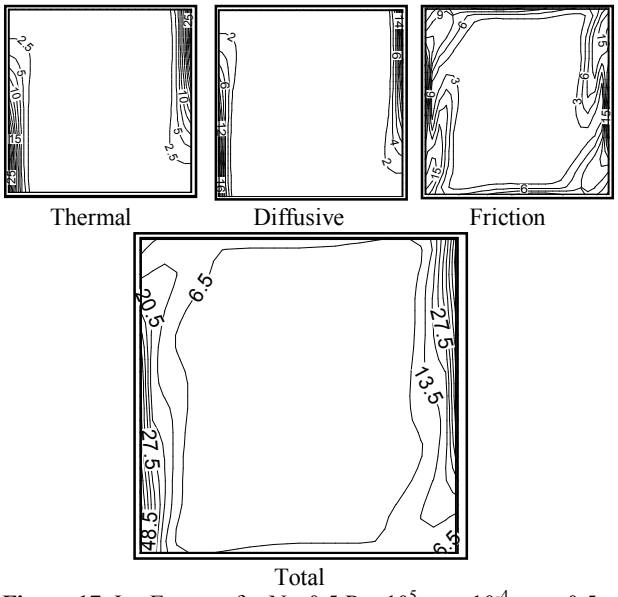

Figure 17. Iso-Entropy for N=-0.5,Ra=10^5, φ_1=10^{-4}, φ_2=0.5 and φ_3=0.01

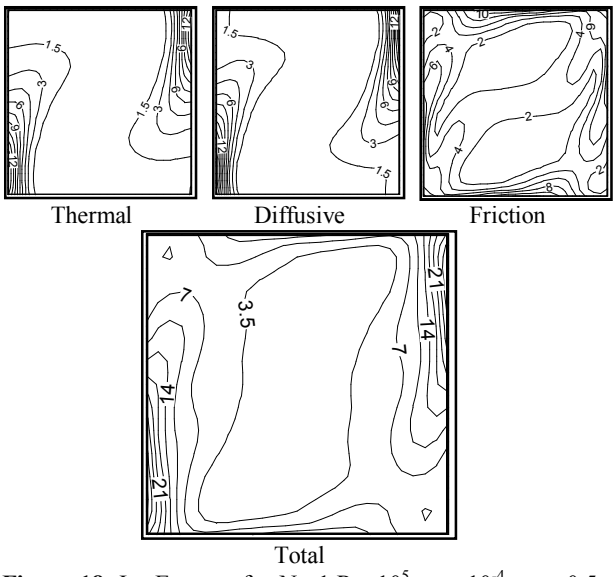

Figure 18. Iso-Entropy for N=-1,Ra=10^5, φ_1=10^{-4}, φ_2=0.5 and φ_3=0.01

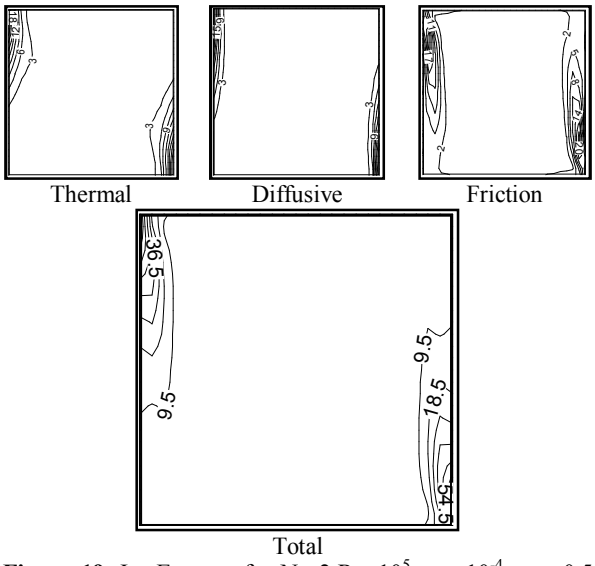

Figure 19. Iso-Entropy for N=-2,Ra=10^5, φ_1=10^{-4}, φ_2=0.5 and φ_3=0.01

Finally, total entropy loses show similar behavior with entropy generation due to fluid friction. As shown in earlier parts, buoyancy ratio plays important role on heat transfer, temperature distribution and fluid flow. As seen from results, the buoyancy ratio is also an effective parameter on entropy distribution. With decreasing value of buoyancy ratio, entropy generation values are also decreased for fixed values of irreversibility distribution ratio as illustrated in Figure 17. Entropy generation for the special case (N = -1) are depicted in Figure 18. As given in the figure, especially very complex structure is obtained for entropy generation due to friction. For values of N = -2, entropy generation becomes less effective on corners as plotted in Figure 19. Effects of fluid friction on entropy generation become lower than that of other parameters as temperature and mass. Figure 20 shows dimensionless entropy generation for different Rayleigh numbers. The graphics are plotted for friction, thermal, diffusive and total entropy generation with different values of buoyancy ratio.

Total entropy generation and entropy generation due to fluid friction follow similar trend for Ra = 10^5 and 10^4. Entropy generation due to fluid friction is almost zero for the lowest value of Rayleigh number due to low velocities and heat transfer. All parameters have minimum values between N = -1.5 and -1 and maximum for N = 1 and 1.5 at Ra = 10^5. Moreover, entropy generation due to fluid friction and total entropy generation become the lowest value than that of entropy generation due to thermal and mass. Finally, Figure 21 illustrates Bejan numbers for studied parameter. It is calculated from Equation (24) and it is a measure of magnitude of the heat transfer and fluid

friction irreversibilities [27-28]. In addition, Be = 1.0 is the limit at which all the irreversibility is due to heat transfer, Be = 0 is the opposite limit at which all the irreversibility is due to fluid friction, and Be = 1/2 is the case in which the heat transfer and fluid friction entropy generation rates are equal. Be >> 1/2 is the case where the irreversibility due to heat transfer dominates, while Be << 1/2 is the case where the irreversibility due to fluid friction dominates. In Figure 21, Bejan number is obtained as 1.0 for Ra = 10^3 and heat transfer irreversibility and fluid friction irreversibilities are almost the same. It makes a high value around N = -1.5 due to complex variation of velocity and others for this value buoyancy ratio. For N > -1.5, Bejan numbers decrease gradually with increasing buoyancy ratio.

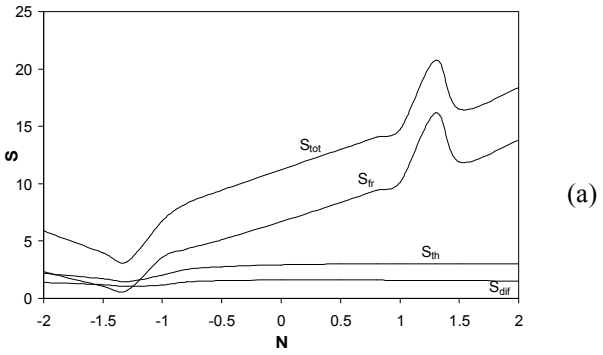

(a)

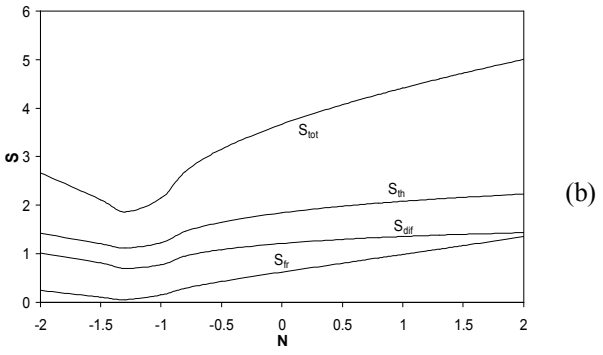

(b)

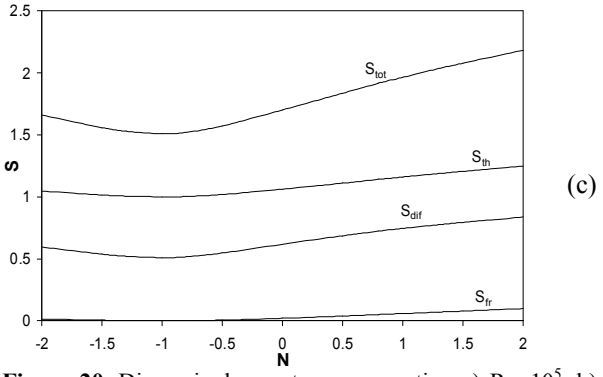

(c)

Figure 20. Dimensionless entropy generation a) Ra=10^5, b) Ra=10^4, c) Ra=10^3

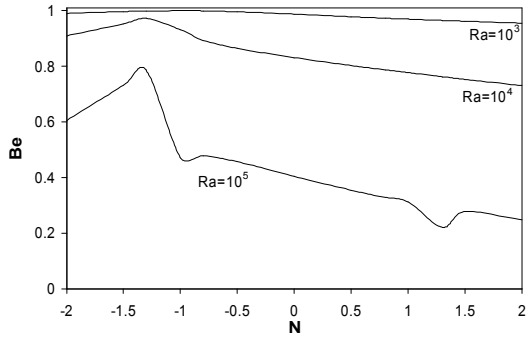

Figure 21. Bejan Number as function of N and different Rayleigh numbers

4. CONCLUSION

A three dimensional numerical study has been done to investigate the heat transfer, mass transfer, fluid flow and entropy generation in a differentially heated cubic enclosure. Effects of Rayleigh number and buoyancy ratio are tested. Important findings can be drawn from this work as listed below:

- Heat and mass transfers and fluid flow are affected from both buoyancy ratio (N) and Rayleigh number (Ra). A specific case is occurred for N values between -1.5 ≤ N ≤ -1. Among these values, flow shows complex structure and it affects entropy generation and heat and mass transfer.
- Entropy generation is good tool to observe energy losses and control of system efficiency.
- Total entropy generation is affected from the buoyancy ratio and it increases with increasing of this value. Entropy generation also increases with Rayleigh number.
- Entropy generation due to fluid friction becomes lower than others for low values of Rayleigh number.
- Bejan number is also calculated in this work. Bejan number decreases with increasing of Rayleigh number and decreases for N > -1.5.

5. REFERENCES

1. Nishimura, T., Wakamatsu, M. and Morega, A. M., "Oscillatory double-diffusive convection in a rectangular enclosure with combined horizontal temperature and concentration gradients", ***International Journal of Heat and Mass Transfer***, Vol. 41, No. 11, (1998), 1601-1611.
2. Wee, H., Keey, R. and Cunningham, M., "Heat and moisture transfer by natural convection in a rectangular cavity", ***International Journal of Heat and Mass Transfer***, Vol. 32, No. 9, (1989), 1765-1778.
3. Bennacer, R., Mohamad, A. A. and Akrour, D., "Transient natural convection in an enclosure with horizontal temperature and vertical solutal gradients", ***International Journal of Thermal Sciences***, Vol. 40, No. 10, (2001), 899-910.

4. Bennacer, R. and Gobin, D., "Cooperating thermosolutal convection in enclosures—i. Scale analysis and mass transfer", ***International Journal of Heat and Mass Transfer***, Vol. 39, No. 13, (1996), 2671-2681.
5. A. Abidi, L. Kolsi, M. N. Borjini, H. Ben Aissia and M. J. Safi, "Effect of heat and mass transfer through diffusive walls on three-dimensional double-diffusive natural convection", ***Numerical Heat Transfer***, Vol. 53, (2008), 1357–1376.
6. Papanicolaou, E. and Belessiotis, V., "Double-diffusive natural convection in an asymmetric trapezoidal enclosure: Unsteady behavior in the laminar and the turbulent-flow regime", ***International Journal of Heat and Mass Transfer***, Vol. 48, No. 1, (2005), 191-209.
7. Beghein, C., Haghighat, F. and Allard, F., "Numerical study of double-diffusive natural convection in a square cavity", ***International Journal of Heat and Mass Transfer***, Vol. 35, No. 4, (1992), 833-846.
8. Sezai, I. and Mohamad, A., "Double diffusive convection in a cubic enclosure with opposing temperature and concentration gradients", ***Physics of Fluids***, Vol. 12, (2000), 2210.
9. Hyun, J. M. and Lee, J. W., "Double-diffusive convection in a rectangle with cooperating horizontal gradients of temperature and concentration", ***International Journal of Heat and Mass Transfer***, Vol. 33, No. 8, (1990), 1605-1617.
10. Goyeau, B., Songbe, J.-P. and Gobin, D., "Numerical study of double-diffusive natural convection in a porous cavity using the darcy-brinkman formulation", ***International Journal of Heat and Mass Transfer***, Vol. 39, No. 7, (1996), 1363-1378.
11. Dakshina Murty, V., "A finite element solution of double diffusive convection", ***International Communications in Heat and Mass Transfer***, Vol. 15, No. 2, (1988), 165-177.
12. Chen, S. and Du, R., "Entropy generation of turbulent double-diffusive natural convection in a rectangle cavity", ***Energy***, Vol. 36, No. 3, (2011), 1721-1734.
13. Han, H. and Kuehn, T. H., "Double diffusive natural convection in a vertical rectangular enclosure—II. Numerical study", ***International Journal of Heat and Mass Transfer***, Vol. 34, No. 2, (1991), 461-471.
14. Reena, and Rana, "Thermosolutal convection of micropolar rotating fluids saturating a porous medium", ***International Journal of Engineering***, Vol. 22, No. 4, (2009), 379-404.
15. Borjini, M. N., Kolsi, L., Daous, N. and Aissia, H. B., "Hydromagnetic double-diffusive laminar natural convection in a radiatively participating fluid", ***Numerical Heat Transfer, Part A: Applications***, Vol. 48, No. 5, (2005), 483-506.
16. Bishnoi, J. and Goyal, N., "Soret dufour driven thermosolutal instability of darcy-maxwell fluid", ***International Journal of Engineering-Transactions A: Basics***, Vol. 25, No. 4, (2012), 367.
17. Bejan, A. and Kestin, J., "Entropy generation through heat and fluid flow", ***Journal of Applied Mechanics***, Vol. 50, (1983), 475.
18. Bejan, A., "Entropy generation minimization: The method of thermodynamic optimization of finite-size systems and finite-time processes", CRC press, Vol. 2, (1996).
19. Bejan, A., "Convection heat transfer", John Wiley & Sons, (2013).
20. Bejan, A., "A study of entropy generation in fundamental convective heat transfer", ***Journal of Heat Transfer***, Vol. 101, (1979), 718.
21. Şahin, A. Z., "Entropy generation in turbulent liquid flow through a smooth duct subjected to constant wall temperature", ***International Journal of Heat and Mass Transfer***, Vol. 43, No. 8, (2000), 1469-1478.
22. Kolsi, L., Abidi, A., Borjini, N. M. and Aïssia, B. H., "The effect of an external magnetic field on the entropy generation in three-dimensional natural convection", ***Thermal Science***, Vol. 14, No. 2, (2010), 341-352.
23. Goni Boulama, K., Galanis, N. and Orfi, J., "Entropy generation in a binary gas mixture in the presence of thermal and solutal mixed convection", ***International Journal of Thermal Sciences***, Vol. 45, No. 1, (2006), 51-59.
24. Varol, Y., Oztop, H. F. and Koca, A., "Entropy production due to free convection in partially heated isosceles triangular enclosures", ***Applied Thermal Engineering***, Vol. 28, No. 11, (2008), 1502-1513.
25. Varol, Y., Oztop, H. F. and Koca, A., "Entropy generation due to conjugate natural convection in enclosures bounded by vertical solid walls with different thicknesses", ***International Communications in Heat and Mass Transfer***, Vol. 35, No. 5, (2008), 648-656.
26. Varol, Y., Oztop, H. F., Koca, A. and Avci, E., "Forecasting of entropy production due to buoyant convection using support vector machines (svm) in a partially cooled square cross-sectional room", ***Expert Systems with Applications***, Vol. 36, No. 3, (2009), 5813-5821.
27. Baytas, A. and Pop, I., "Free convection in oblique enclosures filled with a porous medium", ***International Journal of Heat and Mass Transfer***, Vol. 42, No. 6, (1999), 1047-1057.
28. Baytaş, A., "Entropy generation for natural convection in an inclined porous cavity", ***International Journal of Heat and Mass Transfer***, Vol. 43, No. 12, (2000), 2089-2099.
29. Oliveski, R. D. C., Macagnan, M. H. and Copetti, J. B., "Entropy generation and natural convection in rectangular cavities", ***Applied Thermal Engineering***, Vol. 29, No. 8, (2009), 1417-1425.
30. Magherbi, M., Abbassi, H., Hidouri, N. and Brahim, A. B., "Second law analysis in convective heat and mass transfer", ***Entropy***, Vol. 8, No. 1, (2006), 1-17.
31. Shamsi, M. and Nassab, S. G., "Ivestigation of entropy generation in 3-d laminar forced convection flow over a backward facing step with bleeding", ***International Journal of Engineering-Transactions A: Basics***, Vol. 25, No. 4, (2012), 379.
32. Patankar, S. V., "Numerical heat transfer and fluid flow", Taylor & Francis, (1980).

Entropy Generation of Double Diffusive Natural Convection in a Three Dimensional Differentially Heated Enclosure

CH. Maatki, K. Ghachem, L. Kolsi, M. N. Borjini, H. Ben Aissia

Department of Energetic, University of Monastir, Monastir, Tunisie

P A P E R I N F O

Paper history:
Received 10 April 2013
Accepted in revised form 20 June 2013

Keywords:
Entropy Generation
Double Diffusion
Natural Convection
Energy
Three Dimensional

چکیده

تولید انتروپی یک جابجایی طبیعی ساطع شده دوبل در یک محفظه گرمایی دیفرانسیلی سه بعدی به صورت تحلیلی انجام شده است. دیوارهای عمودی محفظه به صورت دیفرانسیلی گرمادهی شد و دیوارهای دیگر آدیاباتیک هستند. نتایج بدست آمده از طریق غلظت های یکسان، دماهای یکسان، پروژه بردار سرعت، مسیرهای ذرات، پروفایل های سرعت، انتروپی یکسان، عددهای شروود و ناسلت محلی، عددهای شروود و ناسلت متوسط و عددهای بجان در مقادیر مختلف نسبت بویانسی ($-2 \le N \le 2$) و عدد رایلی ($10^3 \le Ra \le 10^5$) نشان داده شده است. عدد لوییس در $Le = 2$ ثابت نگه داشته شد. دریافته شد که هم عدد رایلی و هم نسبت بویانسی نقش مهمی در تولید انتروپی و انتقال گرما و جرم همانند جریان سیال ایفا می کنند. یک مورد خاص بین $-1 \le N \le -1.5$ رخ داد و ساختار پیچیده ای مشاهده شد.

doi: *10.5829/idosi.ije.2014.27.02b.06*